1.8 MARITIME DIFFERENCES BETWEEN WIND DIRECTION AND STRESS: RELATIONSHIPS TO ATMOSPHERIC FRONTS AND IMPLICATIONS

P. Ola G. Persson[1], B. Walter[2], and J. Hare[1]
[1]CIRES/University of Colorado/NOAA/ETL, Boulder, CO
[2]Northwest Research Associates, Bellevue, WA

1. INTRODUCTION

Previous researchers have noted differences between the stress and wind directions in the maritime atmospheric surface layer, which would represent a deviation from expectations based on the Monin-Obukhov Similarity Theory. These differences are suggested to result from either vertical momentum transport by large eddies in a directionally-sheared, baroclinic environment (Geernaert 1988) or from stress effects from sea swell that is oriented differently than the local wind direction (Geernaert 1993; Rieder et al 1994; Grachev et al 2003).

Because of the affect of vertical shear, the first mechanism would produce stress directions that are oriented to the right of the wind direction (looking downwind and down-stress) in situations of warm-air advection and to the left for cold-air advection. Geernaert (1988) shows how this directional difference changes sign as a warm front and a cold front passes an instrumented North Sea platform. In the second mechanism, stress effects from swells affect the part of the covariance spectrum associated with the swell frequencies (Geernaert 1993; Rieder et al 1994), producing a net stress direction between the wind direction and the swell direction. Grachev et al (2003) shows that the wind stress is a vector sum of the 1) pure shear stress aligned with the mean wind shear, 2) wind-wave-induced stress aligned with the direction of the pure wind-sea waves, and 3) swell-induced stress aligned with the swell direction. The swell and wind directions may become different in the vicinity of atmospheric fronts as the swell orientations change much less or more slowly than does the wind direction. Physically, this may result either because the swells move faster than the cold front so post-frontal swell orientations are found ahead of the cold front, or because a cold front moves fast enough to not influence the swells over a long enough time period to change their orientation to that of the winds. Hence, both the baroclinic effects and the swell effects may lead to different orientations of the wind and stress directions near atmospheric fronts, and both mechanisms should produce a systematic change in the sign of this difference from one side of the front to the other.

In this study, we present ship-based data from the Fronts and Atlantic Storm Tracks Experiment (FASTEX; Persson et al 2004) in the wintertime North Atlantic Ocean and aircraft data from the Pacific Landfalling Jets Experiment (PACJET) over the northeast Pacific Ocean to again show that these differences between the stress and wind directions occur systematically over the open ocean in the vicinity of atmospheric fronts, and that these differences change sign from the warm sector to the post-frontal regions. Furthermore, we use low-level, in-situ, and radar aircraft measurements with the NOAA P-3 aircraft and simultaneous QuikScat satellite overpasses to explore the impact of the stress-wind directional differences on wind retrievals from satellite-based scatterometers, which rely on the surface stress field. The results show that the retrieved surface wind directions are in error, the surface directional wind shift across the front is underestimated, and that the derivative fields, such as divergence and vorticity are likely underestimated.

2. OBSERVATIONAL DATA

The Fronts and Atlantic Storm Tracks Experiment (FASTEX) was conducted in the North Atlantic Ocean in January and February 1997. One of the objectives of the NOAA-sponsored measurements aboard the *R/V Knorr* was to obtain measurements of surface sensible heat, latent heat and momentum fluxes during the high-wind events associated with the passage of cyclones and fronts. For these measurements, an ultrasonic anemometer/thermometer (Gill-Solent, R2; 20 Hz sampling rate) and a fast-response infrared hygrometer (Ophir, IR-2000), were mounted on a mast in the bow of the ship. Platform-motion corrections were made using a package of 3-axis accelerometers and rotation rate sensors mounted in a canister in close proximity to the sonic anemometer and the method described by Edson *et al.* (1998). While these measurements provided fluxes from the covariance, inertial dissipation, and bulk techniques, only the covariance technique is able to provide the stress direction, θ_τ, through

$$\theta_\tau = \tan^{-1} (\tau_{cc}/\tau_{sc}) + \theta_u \qquad (1)$$

$$\tau_{sc} = -\rho_a(\overline{u_s' w'}) \quad (2)$$

$$\tau_{cc} = -\rho_a(\overline{u_c' w'}), \quad (3)$$

where τ_{sc} is the covariance stress in the streamwise direction (along the direction of the mean wind, θ_u), τ_{cc} is the covariance stress in the cross-stream direction, u_s and u_c are the streamwise and cross-stream wind components, respectively, w is the vertical velocity, primes denote perturbations from the mean, and ρ_a is the air density.

A T. S. K. Corporation microwave wave-height meter (described at http://www.tsk-jp.com/tska/ index.html) provided by the Bedford Institute of Oceanography was deployed on the bow of the *Knorr* to measure wave statistics at a rate of 2 Hz. This instrument included the downward-looking Doppler radar with a 13° beam width, which sampled a 1.8 m diameter footprint of the ocean surface from its location at the end of a short bowsprit, and a gimbaled vertical accelerometer mounted below decks at the bow on the ship's centerline. A floating thermistor and the ship intake provided two in-situ measurements of the sea-surface temperature. In addition, subjective estimates of sea-surface conditions, including wave and swell heights and directions, were provided by the ship's crew from the bridge at least every four hours. A more detailed description of the instrumentation on the *R/V Knorr* during FASTEX and the data processing is provided by Persson *et al.* (2004).

The Pacific Landfalling Jets Experiment (PACJET) was conducted over the eastern North Paciifc Ocean during January and February of 2001 and 2002. A key platform used during PACJET was the National Ocean and Atmospheric Administration's (NOAA's) P-3 research aircraft. Key measurements from the P-3 aircraft included basic temperature, humidity, and wind information, gust-probe data (three-dimensional wind components and temperature data at 40 Hz), radar wind and reflectivity data from the X-band Doppler tailradar, and dropsonde data. The Doppler radar data, only obtainable in precipitating areas, was processed as described by Jorgensen et al (2003), producing a three-dimensional volume of u, v, w, and reflectivity data with a 1x1 km horizontal resolution and a vertical resolution of 250 m. The data presented in this presentation is primarily from a flight through a front due west of central California on Feb. 19, 2001. This case is also described by Jorgensen *et al.* (2003).

QuikScat satellite data of wind speeds and wind direction at a nominal height of 10 m MSL are available twice per day. The resolution of this data is 25 km. For the case of Feb. 19 the rain-mask was removed, since the rain mask had deleted primarily winds that appear to be correct, and very few data points would have been present in the location of the aircraft. Only a few outliers are seen in the resulting QuikScat wind fields.

3. STRESS-WIND DIRECTION DIFFERENCES

3.1 Frontal Time Series

According to theory (Grachev et al 2003), if the stress is due entirely to wind waves, then the

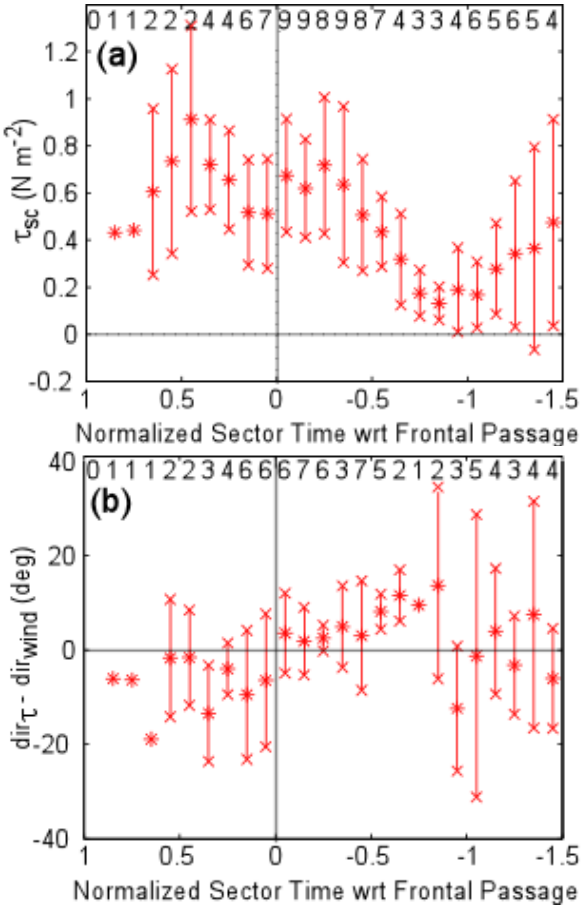

Fig. 1. Composite values of (a) stress and (b) the difference between the stress direction and wind direction with respect to the cold frontal passage from the R/V Knorr for 10 cases during FASTEX. The data were determined from the covariance method. A 3-point running mean was applied to the stress components before the stress direction was calculated. The vertical errors bars show ± one standard deviation.

stress direction should be the same as the wind direction. If other factors, such as the swell, are influencing the stress, then the stress direction should be between the swell and wind directions. Composites of time-series through 10 frontal passages during FASTEX show that the stress direction is often greater than the wind direction by 5-12° (that is, the stress direction is to the right of the wind direction) in the central and western portion of the warm sector east of the surface cold front, while in the post-frontal regime the opposite appears to be true (Fig. 1). In order to do the compositing in Fig. 1, the time has been normalized with the duration of the warm-sector, which is defined as the time from when the surface-layer mixing ratio increases to the time of the cold-frontal passage.

Manual observations of the swell direction show that the warm sector stress direction is frequently between the swell direction and the wind direction, in qualitative agreement with theory (Fig. 2).

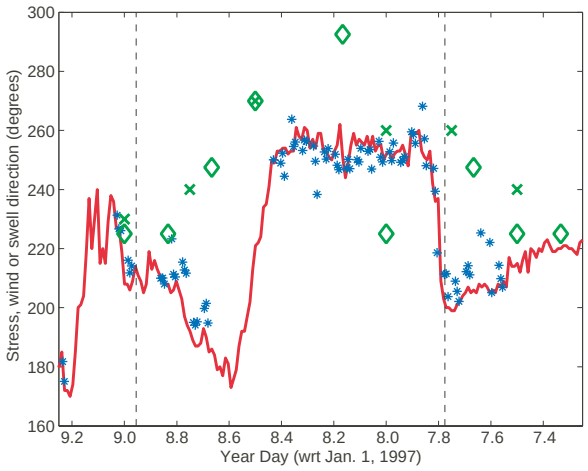

Fig. 2. Time series from the R/V Knorr of wind direction (line), stress direction (*), and manual observations of the swell direction from two different ship logs (diamond, x) for the period Julian Day 7.3 – 9.25. The two vertical dashed lines show the cold-frontal passages for cases 3 and 4.

3.2 Spatial Differences

During PACJET, low-level flight legs with the NOAA P-3 aircraft on both sides of surface cold front of Feb. 19, 2001, showed similar differences between stress and wind directions, both calculated from the aircraft data. Stress directions 150-200 m above the surface were oriented between 6° and 26° to the right of the wind direction east of the cold front while they were up to 26° to the left of the wind direction west of the cold front (Fig. 3). These results from both

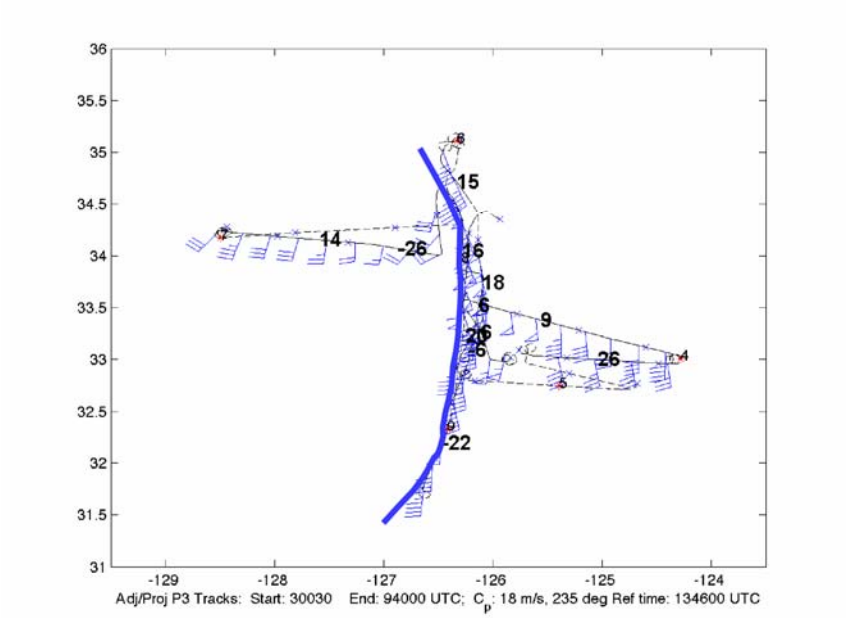

Fig. 3: The difference between the stress direction calculated from the aircraft gust probe data and the aircraft wind direction are shown in bold for 5-10 minute P3 aircraft flux legs below 500 m altitude (solid black lines). Wind barbs are plotted every 4 minutes along the flight track, and the heavy blue line marks the approximate location of the surface cold front. Positive values indicate a more clockwise orientation of the stress vector.

the time series in FASTEX and the quasi-instantaneous measurements from PACJET suggest that in the vicinity of fronts, the stress vector may not be an accurate indicator of the wind direction, either in the warm sector, post-frontal regime, or both. Furthermore, the change in the stress and wind directional differences is systematic across the front, such that the stress direction is to the right of the wind direction in the warm sector ahead of the cold fronts and to the left of the wind direction in the cold air behind the cold fronts..

4. CONSEQUENCE OF DIFFERENCES

Satellite-based scatterometer measurements of the ocean surface, such as those from QuikScat, utilize the surface signatures of the near-surface stress to deduce the surface wind speed and direction. Hence, the scatterometer wind directions are aligned along the stress direction. QuikScat measurements of the surface winds are currently operationally ingested into numerous numerical weather prediction models, in which low-level winds are used to compute dynamically important variables, such as vorticity and divergence. One consequence of the difference between the stress and wind direction and its systematic change across atmospheric fronts is that these QuikScat wind directions may be in error, and the dynamical variables dependent on the wind directions can also be in error because of the systematic way in which the directional errors vary across a front.

Figure 4 shows the QuikScat 10-m wind field from 0255 UTC Feb. 19, 2001. Overlaid on

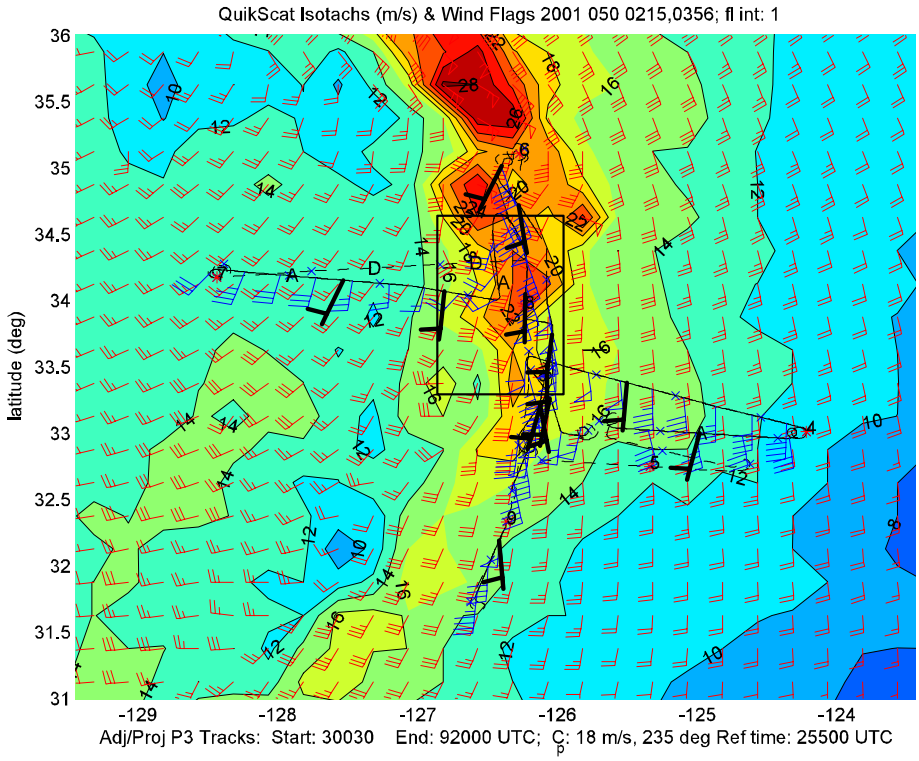

Fig. 4: QuikScat 10-m isotachs overlaid with QuikScat 10-m wind barbs (red), low-level aircraft wind barbs from the NOAA P-3 aircraft (blue), and flight-level stress directions (black barbs). The data are from Feb. 19, 2001. The heavy blue line marks the approximate location of the surface cold front, and the box marks the location of the P-3 radar sampling box shown in Figs. 6 and 8.

this field is the P-3 aircraft flight track from 0410-0830 UTC Feb. 19, time-space adjusted to 0255 UTC using a frontal phase velocity of 18.1 ms-1 from 235. Also shown are the flight-level wind barbs (blue) when the aircraft was below 500 m MSL and the stress direction (black) at these times. The surface cold front lies along the western edge of the high-wind speed zone, which marks the common prefrontal low-level jet.

To directly compare aircraft and QuikScat data, the aircraft in-situ data were averaged for the time the aircraft was located within a QuikScat grid box (typically about 4 minutes). Differences between the average aircraft and corresponding QuikScat data were plotted in Fig. 5 as a function of height for all the corresponding points in the warm sector to the east of the front. A best-fit polynomial is calculated for each profile. As can be seen, the aircraft and QuikScat wind speeds

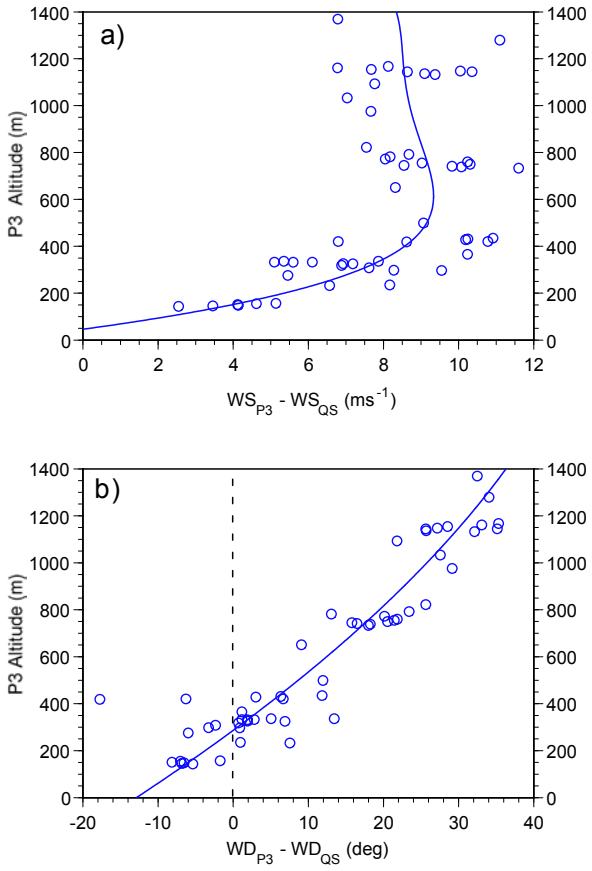

Fig. 5: *Difference between the coincident P-3 aircraft and QuikScat wind speed (a) and wind direction (b) as a function of aircraft altitude for Feb. 19, 2001. Downward extrapolation of the data suggests very little difference in wind speed at the surface but a directional difference of 10-20 degrees.*

are in excellent agreement, with the polynomial extrapolation of the difference at the surface being very close to zero. However, for the wind direction, the difference at the surface is about -13°, indicating that the QuikScat winds have a greater westerly (less easterly) component than the observed winds ahead of the front. This is the same qualitative difference as shown between the stress and the wind directions at flight level in Figs 3 and 4. Similar difference profiles in the post-frontal regime are not possible because the aircraft only flew at one level (305 m). Note that the directional differences between the post-frontal flight level data and the QuikScat winds below (Fig. 4) are qualitatively consistent with backing winds with height in a post-frontal regime and don't necessarily reflect errors in the QuikScat surface winds.

The P-3 Doppler winds are obtained in a 20-30 km wide swath of light-to-heavy precipitation extending about 150 km along the center portion of the cold front (Fig. 6; also see Fig. 4 for location with respect to QuikScat winds). These data can be used to compute the vorticity and divergence fields, as can the QuikScat winds, permitting the possibility of comparing the fields from the two systems. However, the radar Doppler winds are obtained at a much finer resolution than the QuikScat winds, so the radar fields of vorticity and divergence are more than one-order of magnitude larger in magnitude (Figs. 7 and 8). Hence, they

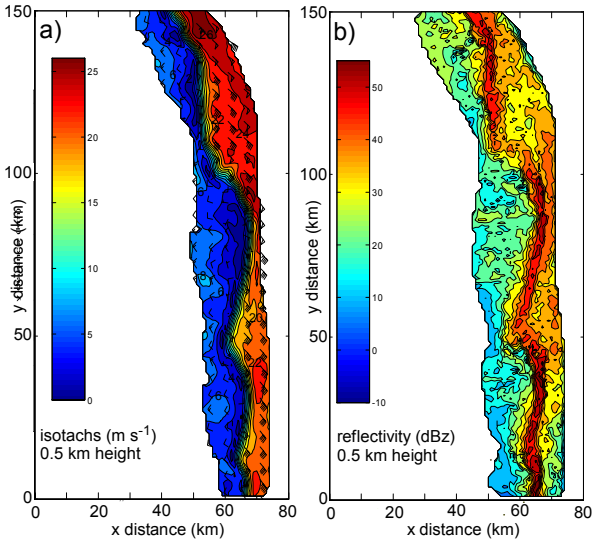

Fig. 6*: P-3 radar analyses at 500 m MSL of a) isotachs (m s^{-1}) and wind barbs, and b) radar reflectivity (dBz) between 0520 and 0554 UTC, Feb. 19, 2001.*

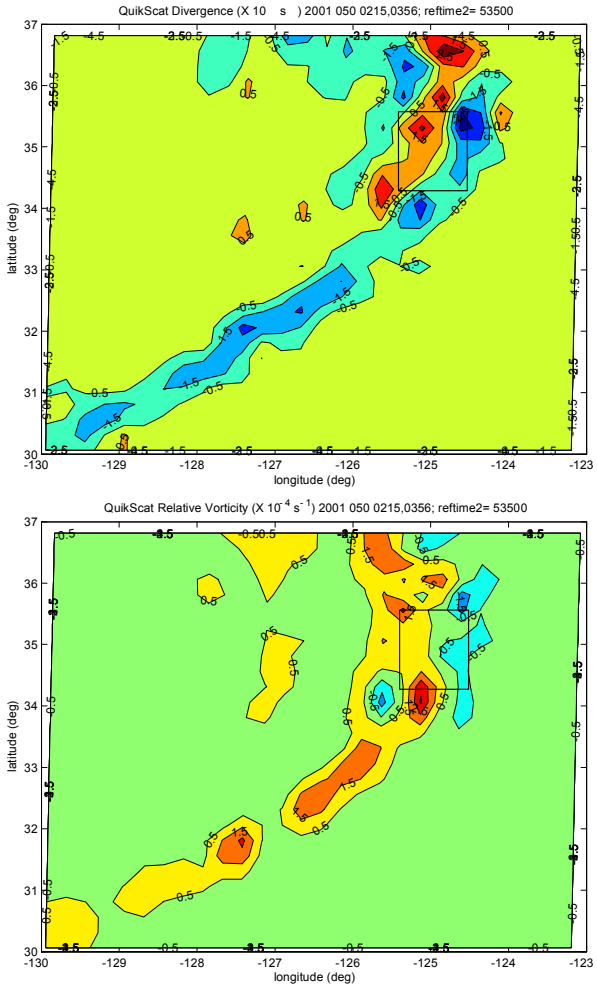

Fig. 7: Fields of a) divergence (X 10-4 s-1) and b) relative vorticity (X 10-4 s-1) derived from the QuikScat satellite winds at 0255 UTC Feb. 19, 2001. The box shows the area of the P-3 tailradar analysis shown in Fig. 8.

can't be directly compared. Therefore, the vorticity and divergence fields from the radar data are computed by averaging the u and v fields to a 25 X 25 km grid before the computation is done. Since the area of winds is only about 20-30 km in the cross-frontal direction, the u and v wind components are assumed to be constant in the E-W direction from the edge of the useable echo into the region of no echos in order to obtain winds with which to compute the vorticity and divergence.

Furthermore, because of the effects of sea-clutter, the Doppler radar winds are only reliable down to about 500 m, while the QuikScat winds only represent the 10-m height. By doing these computations at 5 levels between 500 m and 1.25 km and averaging the fields at each

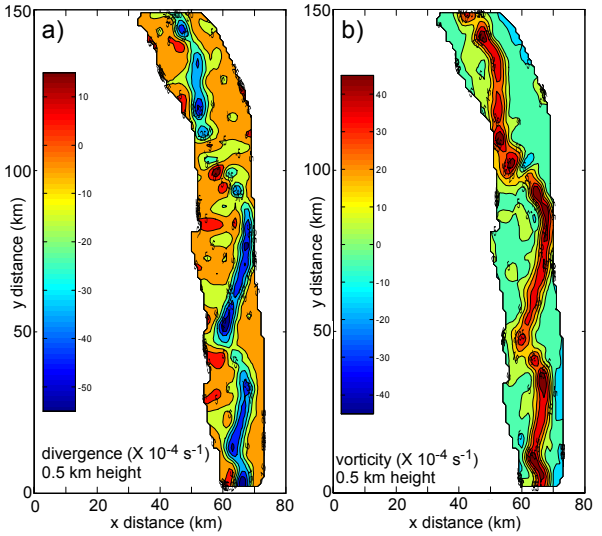

Fig. 8: Fields of a) divergence and b) relative vorticity derived from the 1 km X 1 km P-3 radar data.

level, a vertical profile of vorticity and divergence is obtained and can be extrapolated from 500 m to the surface (Fig. 9). Because of the averaging the u and v fields to 25 km X 25 km grid points, the fields of vorticity and divergence are only two gridpoints in the E-W direction and 5 grid points in the N-S direction, with the number of grid points used in the averages in Fig. 9 varying between 6 and 10 points at the different levels. The vorticity and divergence values for the QuikScat data are the maximum values obtained with 8 adjacent grid points. Both the vorticity and diveregnce maxima were obtained close to the aircarft domains indicated by the boxes in Fig. 7.

Because the fields are computed in the high vorticity and large negative divergence (large convergence) environment of a strong cold front, we expect that the magnitude of the vorticity and divergence profile in Fig. 9 should be a maximum near the surface (e.g., Hobbs and Persson 1982). Since the QuikScat-derived vorticity and divergence fields have much smaller magnitudes than the radar-derived ones at 500 m, this provides strong evidence that the change in the QuikScat-derived surface wind direction is too small across the cold front.

6. CONCLUSIONS

The data from the FASTEX and PACJET field programs over the open ocean indicate that the stress direction is 10-15° to the right of the wind direction (looking downwind and down-stress) in situations before the passage (to the

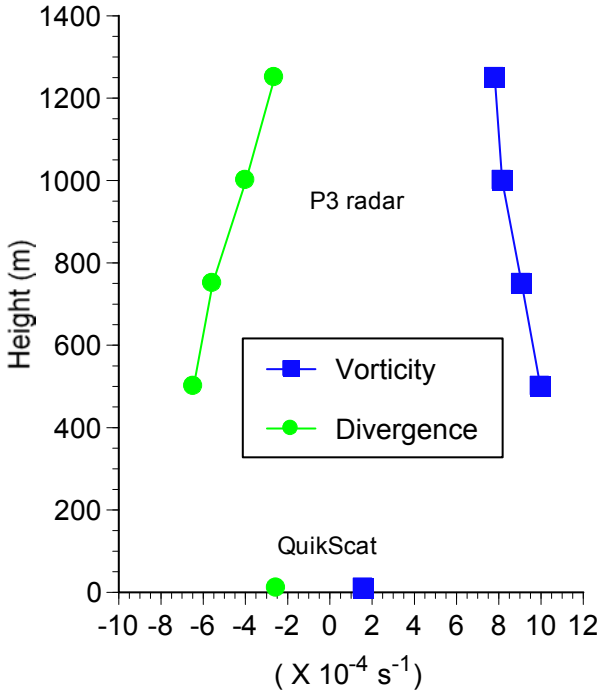

Fig. 9: Average vorticity and divergence along the Feb. 19 cold front from the P-3 radar data between 500 m and 1250 m and from the QuikScat data at 10 m. The radar data is the average of 6-10 coarse grid popints, while the QuikScat data represent the maximum average of 8 points.

east) of cold fronts and a similar amount to the left of the wind direction after the cold-frontal passage. The storms studied are situations of strong winds. These results support previous studies showing similar phenomena, and suggest that these conditions are pervasive.

In this study, we did not explore the cause(s) of these differences in detail, other than providing evidence from FASTEX that swell-induced stress may have caused the differences. However, the location and behaviour of the differences are also consistent with them being generated by vertical transport of momentum by large eddies in a vertically-sheared baroclinic environment.

The presence of these systematic directional differences between stress and wind implies that satellite-based scatterometer wind directions, which rely on the surface stress field, will be in error and will underestimate the surface directional wind shift across the front. Thus the derivative fields, such as convergence and vorticity, will also be underestimated. This study has provided independent evidence of errors in the QuikScat wind directions and of an underestimate of the vorticity and divergence values obtained from the QuikScat data for a strong Pacific cold front.

Future work will utilize the extensive data available for FASTEX and PACJET to try to assess the causes of these differences. Future work on the impacts of these differences will utilize analyses of additional cases where the QuikScat and aircraft data are even closer in time than the 2-3 hours difference for this case.

Acknowledgements

This work was supported by National Aeronautics and Space Administration (NASA) Grant NAG5-10790 and National Science Foundation (NSF) grant ATM-9727054. David Jorgensen kindly provided 3D volumes of aircraft Doppler radar data.

7. REFERENCES

Geernaert, G. L., 1988: Measurements of the angle between the wind vector and wind stress vector in the surface layer over the North Sea. *J. Geophys. Res.*, **93**, 8215-8220.

Geernaert, G. L., F. Hansen, M. Courtney, and T. Herbers, 1993: Directional attributes of the ocean surface wind stress vector. *J. Geophys. Res.*, **98**, 16,571-16,582.

Grachev, A. A., C. W. Fairall, J. E. Hare, J. B. Edson, and S. D. Miller, 2003: Wind stress vector over ocean waves. *J. Phys. Oceanogr.*, **33**, 2408-2429.

Hobbs, P. V., and P. O. G. Persson, 1982: The mesoscale and microscale structure and organization of clouds and precipitation in midlatitude cyclones. Part V: The substructure of narrow cold-frontal rainbands. *J. Atmos. Sci.*, **39**, 280-295.

Jorgensen, David P., Zhaoxia Pu, P. Ola G. Persson, and Wei-Kuo Tao, 2003: Variations associated with cores and gaps of a Pacific narrow cold frontal rainband. *Mon. Wea. Rev.*, **131**, 2705-2729.

Persson, P. Ola G, J. E. Hare, C. W. Fairall, and W. Otto, 2004: Air-sea interaction processes in warm and cold sectors of extratropical cyclonic storms observed during FASTEX. Submitted to *Quart. J. Roy. Meteor. Soc.*

Rieder, K. F, J. A. Smith, and R. A. Weller, 1994: Observed directional characteristics of the wind, wind stress, and surface waves on the open ocean. *J. Geophys. Res.*, **99**, C11, 22,589-22,596.